Effect of Heat Treatment on the Thermoelectric Properties of Bismuth–Antimony–Telluride Prepared by Mechanical Deformation and Mechanical Alloying

DEUK-HEE LEE,[1] JAE-UK LEE,[1] SUNG-JIN JUNG,[1]
SEUNG-HYUB BAEK,[1] JU-HEON KIM,[1] DONG-IK KIM,[1]
DOW-BIN HYUN,[1,2] and JIN-SANG KIM[1,3]

1.—Future Convergence Research Division, Korea Institute of Science and Technology, Seongbuk-gu, Seoul 136-791, Republic of Korea. 2.—e-mail: dbhyun@kist.re.kr. 3.—e-mail: jskim@kist.re.kr

In this work, p-type $20\%Bi_2Te_3$–$80\%Sb_2Te_3$ bulk thermoelectric (TE) materials were prepared by mechanical deformation (MD) of pre-melted ingot and by mechanical alloying (MA) of elemental Bi, Sb, and Te granules followed by cold-pressing. The dependence on annealing time of changes of microstructure and TE properties of the prepared samples, including Seebeck coefficient, electrical resistivity, thermal conductivity, and figure-of-merit, was investigated. For both samples, saturation of the Seebeck coefficient and electrical resistivity were observed after annealing for 1 h at 380°C. It is suggested that energy stored in samples prepared by both MA and MD facilitated their recrystallization within short annealing times. The $20\%Bi_2Te_3$–$80\%Sb_2Te_3$ sample prepared by MA followed by heat treatment had higher a Seebeck coefficient and electrical resistivity than specimens fabricated by MD. Maximum figures-of-merit of 3.00×10^{-3}/K and 2.85×10^{-3}/K were achieved for samples prepared by MA and MD, respectively.

Key words: Bismuth antimony telluride, thermoelectric property, mechanical alloying, mechanical deformation, powder metallurgy

INTRODUCTION

Thermoelectric (TE) cooling modules have been widely used in electronic and optical devices, for example microprocessor chips, high-power laser diodes, light emitting diodes, and infrared detectors, which suffer from severe reliability problems under thermal stress, because of their need for rapid and precise control of temperature and freedom from noise during operation.[1–3] For wide application of TE cooling, high performance and good mechanical reliability of TE materials are required. Current research focuses on these requirements.

Bi_2Te_3–Sb_2Te_3 alloys are the best TE materials, with dimensionless figures-of-merit (ZT, $= S^2\sigma/\kappa$, where S, σ, κ, and T are the Seebeck coefficient,

electrical conductivity, thermal conductivity, and absolute temperature, respectively) of approximately 1.0 for near-room-temperature applications in cooling devices. These alloys have a remarkable anisotropy, which originates from a rhombohedral structure composed of quintuple atomic layer series in the order $Te^{(1)}$–Bi (or Sb)–$Te^{(2)}$–Bi (or Sb)–$Te^{(1)}$ along the c-axis.[4] Bi_2Te_3–Sb_2Te_3 alloys are usually prepared by unidirectional crystal growth methods, for example zone melting or Bridgman technology.[4,5] Although the resulting single-crystal materials have excellent TE properties, their mechanical properties are poor, because of weak Van der Waals bonding between the $Te^{(1)}$–$Te^{(1)}$ layers. Because a combination of good TE and good mechanical properties is required, powder metallurgical and sintering methods, which produce randomly oriented polycrystalline microstructure and thus good mechanical properties, for example mechanical

alloying (MA), sintering of pulverized and inter-mixed elements, hot extrusion, hot-pressing, and cold-pressing with mechanical deformation (MD), have been extensively studied.[6–10] However, TE properties are very sensitive to the conditions used for fabrication, for example powder oxidation in MA and generation of defects by plastic deforma-tion.[11,12] The effects of deformation-induced defects on the TE properties of pure Bi_2Te_3 were reported by Schultz et al.[13] They found that lattice defects acting as donors were introduced by severe defor-mation, for example extrusion and pressing.

In the Bi_2Te_3–Sb_2Te_3 pseudo-binary system, the TE properties of the 20%Bi_2Te_3–80%Sb_2Te_3 compo-sition are known to result in the best performance in terms of ZT.[14,15] In the work discussed in this paper, we compared the TE properties of polycrys-talline p-type 20%Bi_2Te_3–80%Sb_2Te_3 materials prepared by use of different fabrication meth-ods—MD of the as-solidified ingot and MA of ele-mental Bi, Sb, and Te granules followed by heat treatment. The dependence on annealing time of changes of microstructure and TE properties, including the Seebeck coefficient, electrical resis-tivity, thermal conductivity, and figure-of-merit, were also investigated.

EXPERIMENTAL PROCEDURES

To study the effect of MD on TE properties, a 20%Bi_2Te_3–80%Sb_2Te_3 ingot was prepared from pure (99.999%) Bi, Sb, and Te granules as starting materials. The materials were weighed in the appropriate atomic ratios then melted in an evac-uated quartz tube by use of a rocking furnace at 750°C for 5 h to prepare an homogeneous ingot. Specimens ($5 \times 5 \times 12$ mm^3) were cut from the solidified ingot and deformed by cold-pressing at 700 MPa from 1 to 10 times. To maximize the MD, the cold-pressed specimen was removed from the mold then replaced upright in the mold after each pressing step. By this method we prevented oxida-tion of cold-pressed pellets as a result of exposure to the atmosphere.

To prepare 20%Bi_2Te_3–80%Sb_2Te_3 alloy powders by MA, appropriate amounts of Bi, Sb, and Te were weighed and placed in a steel vial with steel balls as milling media. Ball-to-material weight ratio was 5:1. MA was conducted by rotating the vial at approximately 1200 rpm for 6.5 h by use of a SPEX mixer and mill. The powders prepared by MA were cold-pressed at 700 MPa to form $5 \times 5 \times 12$ mm^3 pellets.

The cold-deformed pellets were annealed at 380°C in an evacuated quartz tube. After specific isother-mal annealing times the specimens were cooled to room temperature and their TE properties were measured, to monitor changes in the properties and microstructure during the course of the heat treatment.

The Seebeck coefficient was measured by a static dc method based on the slope of a voltage versus temperature-difference curve, by use of commercial equipment (TEP600; Seepel, Korea). Electrical resistivity was measured by the four-point current-switching method. Thermal conductivity was determined by the Harman method and directly measured by use of the laser flash method (LFA 447, Netzsch Korea, Korea); the two sets of measure-ments were within ±5% of each other.

X-ray diffraction (XRD) patterns of the quenched ingot and compacted pallets after cold-pressing or annealing were obtained by use of an x-ray diffrac-tometer (D8 Discover; Bruker AXS Korea, Korea) with CuKα radiation and a step/time scan mode of 0.01°/1 s. The microstructure was analyzed by electron back scatter diffraction (EBSD) (Quantax EBSD e-Flash^{1000}; Bruker AXS Korea) in an Hitachi S-4300 FEG-SEM (Hitachi High-Tech Korea, Korea).

RESULTS AND DISCUSSION

Figure 1 shows XRD patterns obtained from the as-solidified ingot and from samples prepared by MA and MD, obtained from a section perpendicular to the pressing direction. The peak intensities were normalized to the (015) diffraction peak. The peaks obtained from all the samples were a good match with the standard pattern of rhombohedral 20%Bi_2Te_3–80%Sb_2Te_3 alloys (JCPDS #72-1836). For the samples prepared by MD, the relatively high intensity of (00ℓ) peaks, for example (006), (009), (0015), and (0018), is indicative of predomi-nant alignment of the grains along the $[00\ell]$ direc-tion, i.e., the severity of MD is sufficient to cleave the c-planes of the alloys, in which Te$^{(1)}$ and Te$^{(1)}$ atoms are bonded by weak Van der Waals forces, and align them predominantly perpendicular to the pressing direction. The full width at half maximum (FWHM) of the (015) diffraction peaks for pellets prepared by MA and MD, shown in the inset of Fig. 1, is broader than for the as-solidified ingot, indicating that fine grain-sized particles are formed. After annealing process, it was observed that the originally strong intensity of (00ℓ) peaks of the MD sample was suppressed. This indicates that the ab-oriented grains are randomly re-arranged by recrystallization during the annealing process. In addition, the FWHM of (015) peak for the annealed samples prepared by MA and MD became narrow, because grain size was increased. Grain sizes for as-solidified ingot and for annealed samples pre-pared by MA and MD, determined by use of Debye–Scherrer equation, were 8.83 μm, 5.92 μm, and 7.28 μm, respectively.

The effect of the different manufacturing pro-cesses on the Seebeck coefficient and electrical resistivity of the samples is summarized in Table I. The as-solidified ingot had a Seebeck coefficient of 123 μV/K and an electrical resistivity of 1.2 mΩ cm.

For the pellets prepared by MD, the electrical resistivity increased from $\sim$1.5 mΩ cm to $\sim$2.5 mΩ cm and the Seebeck coefficient increased slightly and remained constant with increasing number of cold-pressing processes. During MD, not only cleavage along the basal planes but also substantial plastic flow on nonbasal planes might produce point defects as a result of dislocation intersections. Schultz et al.[13] suggested that tellurium vacancies, which are generated by MD, are the dominant defects, and are electrically negative carriers. Hence, the increase in electrical resistivity

with increasing MD might reflect the decrease in carrier concentration because of compensation by introduced defects, and the decrease in carrier mobility with decreasing grain size. The cold-pressed pellet prepared by MA had higher Seebeck coefficient and electrical resistivity than the specimen prepared by MD, as shown in Table I.

Figure 2 shows the EBSD images for samples mechanically deformed and annealed 10 times. Dark areas in Fig. 2a are a result of lattice distortions, for example dislocations and vacancies. The image of the as-deformed sample in Fig. 2a is indicative of an unclear grain structure; it is, however, readily apparent that annealing led to dynamic recrystallization within 10 min and a significant increase of grain size for samples mechanically deformed 10 times. The change of the microstructure during annealing may cause changes in TE properties, for example electrical resistivity and Seebeck coefficient.

Figure 3 shows changes of Seebeck coefficient, electrical resistivity, thermal conductivity, and figure-of-merit for mechanically deformed samples with annealing time at 380°C. The Seebeck coefficient, thermal conductivity, and figure-of-merit increase with annealing time. The behavior of electrical resistivity is quite different, however. It increases sharply during initial annealing then rapidly decreases followed by saturation to an equilibrium value.

It is well known that recovery occurs before recrystallization for heavily deformed materials. Schultz et al.[13] reported that MD can introduce both anion and cation vacancies into the sample and those vacancies interact with anti-structural defects and result in compensation of high p-type carriers during the recovery process. Thus, the sharp increase of the electrical resistivity during the initial stage of annealing in Fig. 3b can be explained by the decrease of hole concentration.

The next stage of the annealing process should be recrystallization and grain growth. The recrystallized grains are known to have few dislocations, and hence carrier mobility should increase with grain growth, contributing to reducing the electrical resistivity, as shown in Fig. 3b. However, because the annealing treatment in this work was
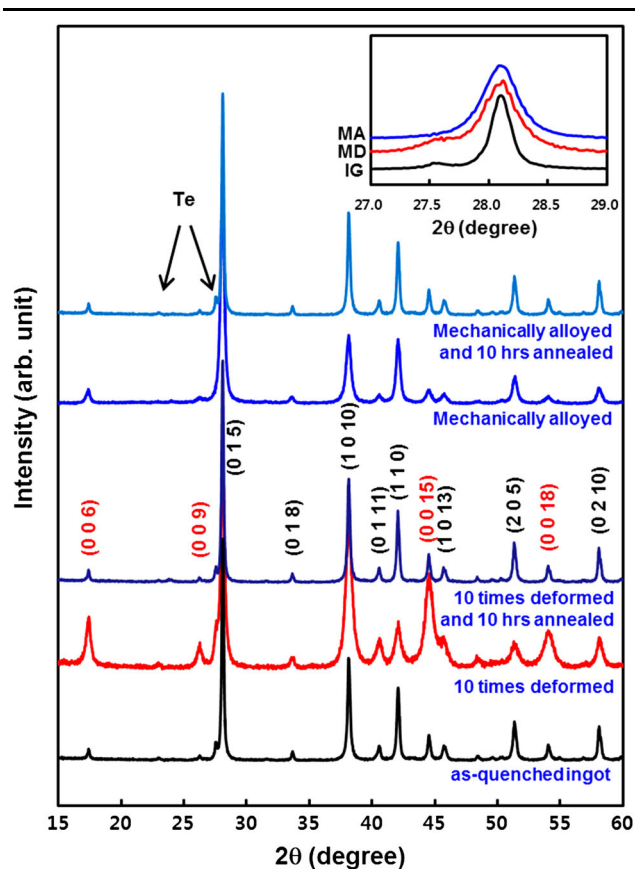

Fig. 1. XRD patterns of mechanically deformed and mechanically alloyed 20%Bi$_2$Te$_3$–80%Sb$_2$Te$_3$ including those annealed at 380°C for 10 h. The inset shows (015) peaks of as-solidified ingot (IG) and 10 times MD and MA samples.

Table I. Room-temperature TE properties of as-solidified ingot, and mechanically deformed and mechanically alloyed 20%Bi$_2$Te$_3$–80%Sb$_2$Te$_3$

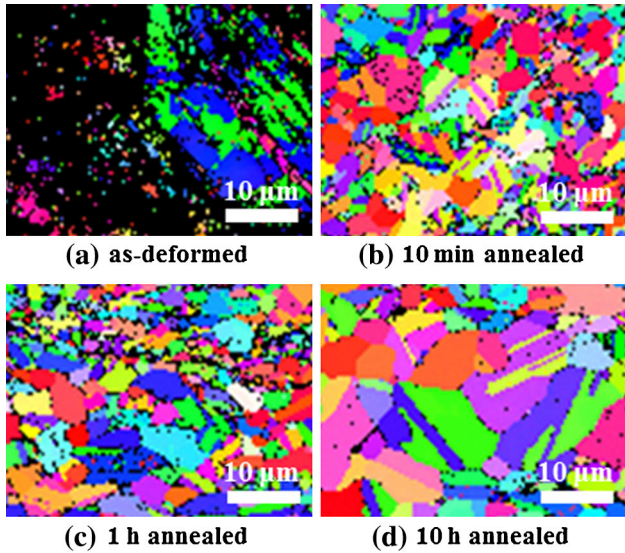|	Seebeck coefficient (μV/K)	Electrical resistivity (mΩ cm)
As-solidified ingot	122.9	1.209
Mechanical deformation		
Number of cold-presses		
2	131.2	1.525
5	132.4	1.860
10	133.4	2.492
Mechanical alloying	156.4	5.060

Fig. 2. EBSD images of mechanically deformed 20%Bi$_2$Te$_3$–80%Sb$_2$Te$_3$ alloys annealed at 380°C: (a) as-deformed, (b) annealed for 10 min, (c) annealed for 1 h, and (d) annealed for 10 h.

performed in the (δ+Te) mixture region of the phase diagram, the matrix of the mechanically deformed ingot will be separated into a new δ-phase, which is equilibrated at the annealing temperature, and free tellurium.[16,17] Poudel et al.[18] have reported pure Te precipitates with 5–30 nm size in p-type nanocrystalline (Bi,Sb)$_2$Te$_3$ bulk alloys processed by hotpressing of nanopowders. In Fig. 1, the peaks at 23.0° and 27.6° are believed to be (100) and (101) of pure Te (JCPDS #89-4899). In general, the solidus line of the δ-phase in p-type (Bi,Sb)$_2$Te$_3$ alloys shifts to the Te-rich side on lowering the temperature; the hole concentration of the recrystallized δ-phase is lower than that of the as-solidified ingot, i.e., the Seebeck coefficient of the recrystallized δ-phase is higher than that of the ingot. Thus, the increase of the Seebeck coefficient with annealing time for the 10 times mechanically deformed samples, shown in Fig. 3a, can be explained on the basis of conversion of the deformed ingot matrix to newly recrystallized δ-phase. Reaching the maximum value means that recrystallization is complete and only grain growth
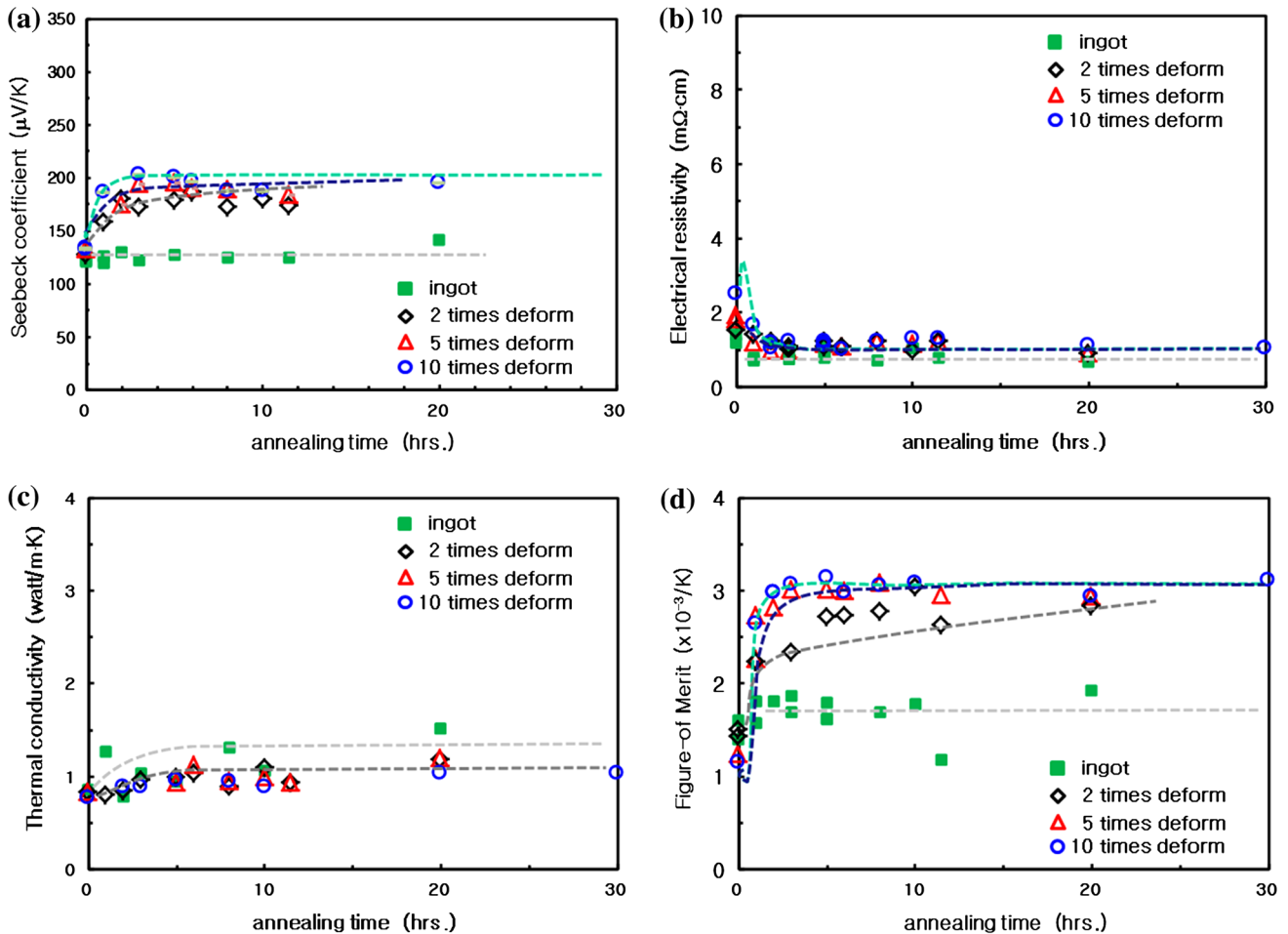

Fig. 3. (a) Seebeck coefficient, (b) electrical resistivity, (c) thermal conductivity, and (d) figure-of-merit of the as-solidified ingot and mechanically deformed 20%Bi$_2$Te$_3$–80%Sb$_2$Te$_3$ alloys as a function of annealing time at 380°C.

Effect of Heat Treatment on the Thermoelectric Properties of Bismuth–Antimony–Telluride Prepared
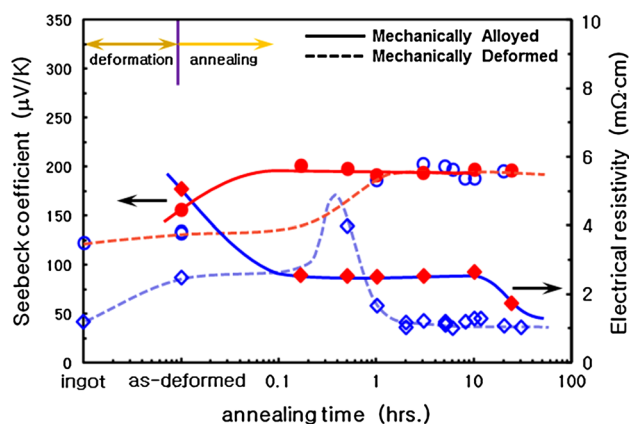by Mechanical Deformation and Mechanical Alloying

2259

Fig. 4. Change of Seebeck coefficient and electrical resistivity with annealing time at 380°C for 20%Bi_2Te_3–80%Sb_2Te_3 alloys prepared by MA. Data from Fig. 3a and b are also included for comparison.
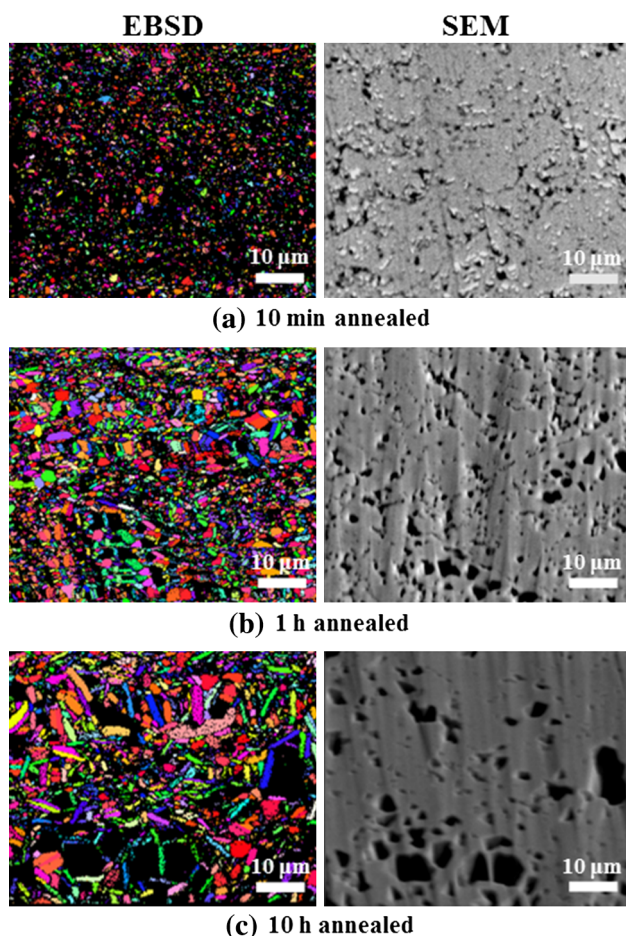

(a) 10 min annealed

(b) 1 h annealed

(c) 10 h annealed

Fig. 5. EBSD and SEM images of 20%Bi_2Te_3–80%Sb_2Te_3 alloys prepared by MA and annealed at 380°C: (a) annealed for 10 min, (b) annealed for 1 h, and (c) annealed for 10 h.

occurs, because the Seebeck coefficient is little affected by grain size and orientation.

Figure 4 shows the change of Seebeck coefficient and electrical resistivity with annealing time at

380°C for alloys prepared by MA. The changes for samples prepared by MD (same as Fig. 3a and b) are also plotted for comparison. EBSD and SEM images for samples prepared by MA with different annealing time are shown in Fig. 5. Basically, a similar trend of Seebeck coefficient and electrical resistivity as a function of annealing time is observed for samples prepared by both MA and MD: they become saturated by annealing. However, there are two distinct features. First, the saturated values of the Seebeck coefficient and the electrical resistivity are different: samples prepared by MA have higher Seebeck coefficient and electrical resistivity than samples prepared by MD. Second, the rate of saturation is also different: TE properties of samples prepared by MA approach saturation values faster than those of samples prepared by MD. This might be because of the high internal energy of samples prepared by MA, in the form of defects such as a high density of dislocations and a large number of grain boundaries, because grain size for powders prepared by MA is much smaller than that for powders prepared by MD. Such high internal energy can act as an extra source of energy driving the material into an equilibrium state. Recrystallization and grain growth during thermal annealing are also observed for the samples prepared by MA, shown in Fig. 5. It is noted that grain growth for samples prepared by MA is quite suppressed compared with that for samples prepared by MD. This might be because of the grain boundary pinning effect of pores in samples prepared by MA, as shown in Fig. 5. Further examination is needed to identify the exact reason.

Annealing in the temperature range from 300°C to 550°C was also performed for alloys prepared by MA and MD. For temperatures higher than 400°C, i.e., higher than the eutectic temperature we applied a hot-press for the cold-pressed pellets instead of vacuum sealed annealing. The resulting equilibrated values are summarized in Fig. 6. The Seebeck coefficient and electrical resistivity decrease with increasing annealing temperature, as shown in Fig. 6a, b. Throughout the temperature range, the Seebeck coefficient of samples prepared by MA is slightly higher than that of samples prepared by MD, probably because of oxidation of the powders prepared by MA. As discussed in relation to Fig. 4, oxygen is a donor dopant, reducing hole carrier concentration, thus the electrical resistivity of samples prepared by MA was also higher than that of samples prepared by MD, as shown in Fig. 6b. The thermal conductivity seems to decrease with increasing annealing temperature when annealed below 400°C. However, thermal conductivity is slightly increased when the annealing temperature is >400°C, because of enhancement of the phonon mean-free-path by the large grain size obtained as a result of high-temperature annealing. All the samples prepared by MA had lower thermal conductivity than those prepared by MD, probably
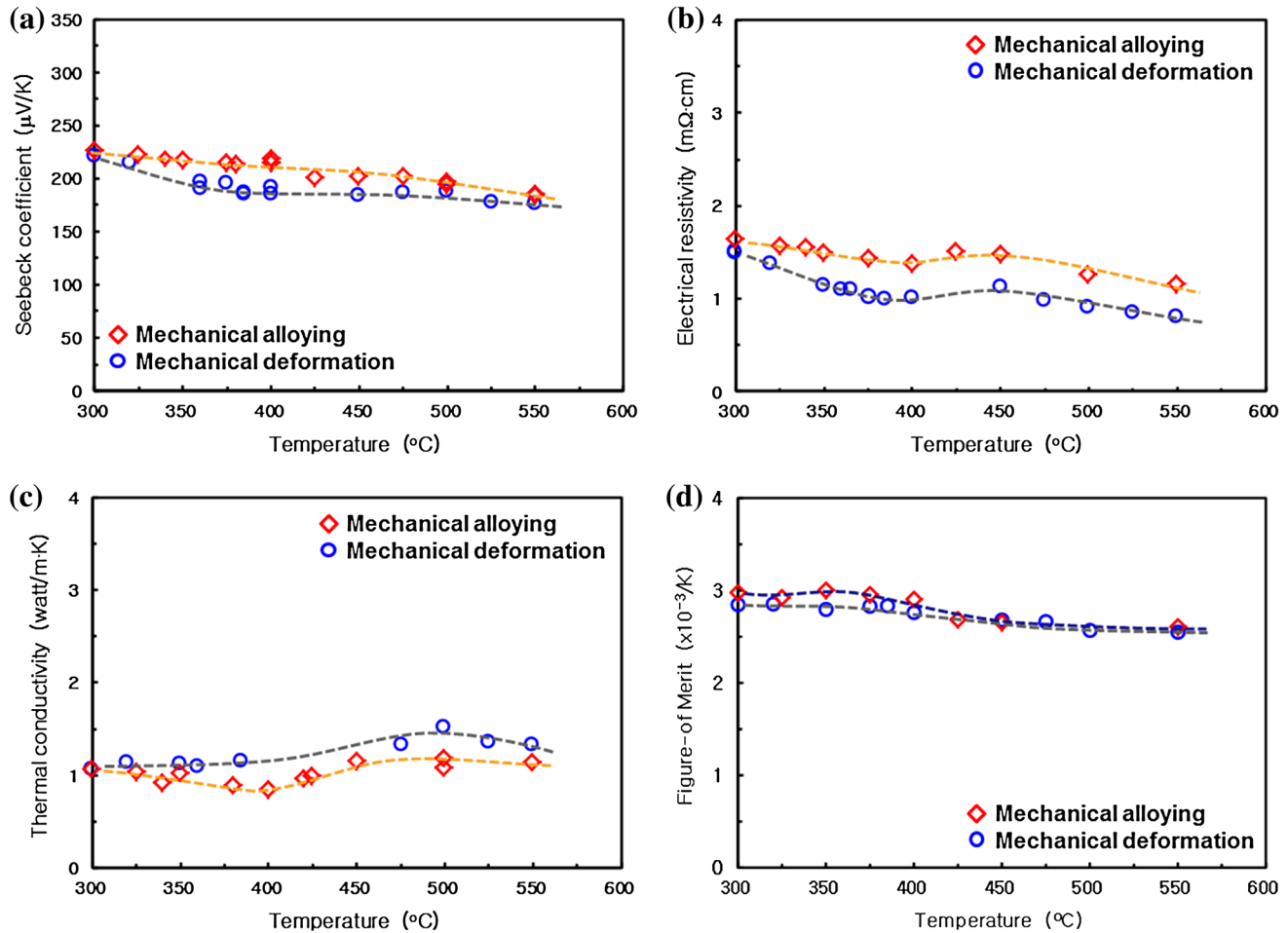
Fig. 6. Temperature-dependence of (a) Seebeck coefficient, (b) electrical resistivity, (c) thermal conductivity, and (d) figure-of-merit for 20%Bi_2Te_3–80%Sb_2Te_3 alloys prepared by MD and MA.

because of phonon scattering at the grain boundaries. The maximum figure-of-merit of samples prepared by MA and MD were 3.00×10^{-3}/K and 2.85×10^{-3}/K, respectively, at annealing temperatures of approximately 350°C.

CONCLUSIONS

In this study, p-type 20%Bi_2Te_3–80%Sb_2Te_3 bulk TE materials were obtained by MD of the pre-melted ingot and MA followed by cold-pressing and annealing. The dependence on annealing time of changes of microstructure and TE properties, including Seebeck coefficient, electrical resistivity, thermal conductivity, and figure-of-merit, was investigated for both samples. The relatively high intensity of (00ℓ) peaks for samples prepared by MD is indicative of preferential alignment of grains along the $[00\ell]$ direction, i.e. c-planes are cleaved and aligned preferentially perpendicular to the pressing direction. For pellets prepared by MA and MD, the FWHM of (015) diffraction peaks becomes broader than for the as-solidified ingot, indicating that fine grain-sized particles are formed, and that the residual stress might be stored in the grains. The trend of the Seebeck coefficient and electrical resistivity as a function of annealing time was similar for samples prepared by both MA and MD: they become saturated by annealing. Seebeck coefficient and electrical resistivity were higher for samples prepared by MA than for those prepared by MD. We believe this can be attributed to possible oxidation during MA. The maximum figure-of-merit of samples prepared by MA and MD and annealed at 350°C were 3.00×10^{-3}/K and 2.85×10^{-3}/K, respectively.

Here, we introduce simple and cost-effective method for manufacture of Bi_2Te_3–Sb_2Te_3 based TE materials—MD of the melted ingot followed by annealing. The method can be used to fabricate high-performance TE bulk materials without the difficulties involved in the powder method. Higher TE performance could be expected by optimization of composition and adjustment of the microstructure.

REFERENCES

1. L.E. Bell, *Science* 321, 1457 (2008).
2. C.A. Gould, N.Y.A. Shammas, S. Grainger, and I. Taylor, *Mater. Sci. Eng. B* 176, 316 (2011).
3. I.-Y. Huang Jr, -C. Lin, K.-D. She, M.-C. Li, J.-H. Chen, and J.-S. Kuo, *Sens. Actuators A* 148, 176 (2008).
4. D.B. Hyun, T.S. Oh, J.S. Hwang, J.D. Shim, and N.V. Kolomoets, *Scr. Mater.* 40, 49 (1999).
5. O. Yamashita, S. Tomiyoshi, and K. Makita, *J. Appl. Phys.* 93, 368 (2003).
6. S. Miura, Y. Satob, K. Fukuda, K. Nishimura, and K. Ikeda, *Mater. Sci. Eng. A* 277, 244 (2000).
7. J. Yang, T. Aizawa, A. Yamamoto, and T. Ohta, *J. Alloys Compd.* 309, 225 (2000).
8. J. Yang, T. Aizawa, A. Yamamoto, and T. Ohta, *Mater. Chem. Phys.* 70, 90 (2001).
9. S.J. Hong and B.S. Chun, *Mater. Sci. Eng. A* 356, 345 (2003).
10. H. Kitagawa, T. Nagamori, T. Tatsuta, T. Kitamura, Y. Shinohara, and Y. Noda, *Scr. Mater.* 49, 309 (2003).
11. T.S. Oh, D.B. Hyun, and N.V. Kolomets, *Scr. Mater.* 42, 849 (2000).
12. D.M. Lee, C.H. Lim, D.C. Cho, Y.S. Lee, and C.H. Lee, *J. Electron. Mater.* 35, 360 (2006).
13. J.M. Schultz, J.P. Mchugh, and W.A. Tiller, *J. Appl. Phys.* 33, 2443 (1962).
14. D. Li, R.R. Sun, and X.Y. Qin, *Intermetallics* 19, 2002 (2011).
15. X.-D. Liu and Y.-H. Park, *Mater. Trans.* 43, 681 (2002).
16. D.-B. Hyun, J.-S. Hwang, J.-D. Shim, and T.-S. Oh, *J. Mater. Sci.* 36, 1285 (2001).
17. D.-B. Hyun, T.-S. Oh, J.-S. Hwang, and J.-D. Shim, *Scr. Mater.* 44, 455 (2001).
18. B. Poudel, Q. Hao, Y. Ma, Y. Lan, A. Minnich, B. Yu, X. Yan, D. Wang, A. Muto, D. Vashaee, X. Chen, J. Liu, M.S. Dresselhaus, G. Chen, and Z. Ren, *Science* 320, 634 (2008).